

# ENSO and IOD influence on Indonesian Throughflow variability in the Makassar Strait and Banda Sea

*Siti Khadijah Srioktoviana*<sup>1</sup>, *Mukti Zainuddin*<sup>1\*</sup>, *Musbir Musbir*<sup>1</sup>, *Muzzneena Ahmad Mustapha*<sup>2</sup>, *St. Aisjah Farhum*<sup>1</sup>, *Rachmat Hidayat*<sup>1</sup>, *Alfira Yuniar*<sup>1</sup>

<sup>1</sup>Department of Fisheries Science, Faculty of Marine Science and Fisheries, Hasanuddin University, Perintis Kemerdekaan Km. 10 Street, 90245 South Sulawesi, Makassar, Indonesia

<sup>2</sup>Faculty of Science and Technology. Universiti Kebangsaan Malaysia. 43600 UKM, Bangi Selangor, Malaysia

**Abstract.** The Indonesian Throughflow (ITF) is a critical component of global ocean circulation, yet its response to simultaneous climate phenomena remains complex. This study examines the influence of El Niño-Southern Oscillation (ENSO) and Indian Ocean Dipole (IOD) on oceanographic anomalies in the Makassar Strait and Banda Sea from 2021 to 2024. Satellite data for sea surface temperature (SST), chlorophyll-a (Chl-a), sea surface salinity (SSS), and surface current velocity (CUR) were analyzed to identify spatial distribution patterns during different climate phases. During La Niña, positive SST anomalies were observed due to strengthened ITF warm water transport and reduced upwelling. Conversely, during El Niño–IOD+ phases, SST anomalies were more localized, and Chl-a concentrations significantly decreased, particularly in the Banda Sea. Statistical analysis revealed that ENSO has a strong negative correlation with Chl-a ( $r = -0.58$ ) and a strong positive correlation with CUR ( $r = 0.68$ ) in the Makassar Strait. The findings highlight that ENSO and IOD act as primary drivers of regional oceanographic variability, significantly altering the biological and physical characteristics of the ITF corridors.

**Keywords:** Indonesian Throughflow, ENSO, IOD, ocean circulation, climate variability

## 1 Introduction

Global climate variability phenomena, such as the El Niño-Southern Oscillation (ENSO) and Indian Ocean Dipole (IOD), exert a substantial influence on tropical oceanographic processes in the Indonesian region [1]. Variations in ENSO and IOD phases modulate anomalies in SST, sea level, and upwelling intensity, particularly in southern Indonesian waters [2]. One

---

\* Corresponding author: [mukti@unhas.ac.id](mailto:mukti@unhas.ac.id)

critically affected ocean circulation system is the ITF, which transports warm Pacific water into the Indian Ocean [3, 4].

This study focuses on two critical corridors of the ITF: the Makassar Strait and Banda Sea. The Banda Sea, located in eastern Indonesia, serves as the convergence zone for water masses from the Seram Sea, Flores Sea, and Timor Sea, and functions as the primary exit conduit of the ITF toward the Timor Sea and the Indian Ocean [5]. In contrast, the Makassar Strait represents the principal entry into the Banda Sea [6]. Both corridors share the common role of facilitating ITF transport and are highly susceptible to global climate variability, particularly ENSO and IOD [7]. Nevertheless, their oceanographic characteristics diverge: the Makassar Strait features a relatively narrow north-south current strongly influenced by western Pacific conditions, while the deep basin morphology of the Banda Sea supports enhanced vertical mixing and more complex water mass dynamics [4, 5].

The linkage between ENSO and IOD with the ITF has been widely recognized, as variations in ITF velocity and transport volume can induce anomalies in oceanographic parameters along their pathways [1]. During El Niño events, the ITF typically weakens because of the reduced pressure gradient between the Pacific and Indian Oceans, whereas La Niña conditions tend to strengthen flow [8]. In the context of local oceanography, changes in ITF strength influence the distribution of sea surface temperature (SST), sea surface salinity (SSS), and even chlorophyll-a concentration (Chl-a) in both the Banda Sea and Makassar Strait, which in turn affects marine ecosystems and fisheries productivity [9, 10].

Although previous studies have examined the impact of ENSO–IOD on Indonesian seas and the ITF, most have focused on broad regional scales [10, 11], individual parameters such as SST or Chl-a [12–14], or long-term climatological trends [6]. Comparative assessment of multiparameter oceanographic anomalies across both the upstream ITF entry (Makassar Strait) and downstream deep-basin outflow region (Banda Sea) remains limited [3–5]. Moreover, the effects of recent extreme climate events, such as the 2021–2023 multi-year La Niña and–2023–2024 El Niño–IOD+ co-occurrence, have not been comprehensively analyzed. This study addresses these gaps by integrating four key oceanographic variables (SST, Chl-a, SSS, and surface current velocity (CUR)) to provide an updated and spatially explicit assessment of how these two interconnected ITF respond to ENSO–IOD variabilities.

Therefore, this study aimed to examine the influence of ENSO and IOD variability on anomalies in oceanographic parameters, including SST, SSS, Chl-a, and CUR in the Banda Sea and Makassar Strait. The analysis sought to identify the response patterns of these two regions to global climate variability and to elucidate the mechanisms linking ENSO–IOD events, ITF, and local oceanographic conditions.

## 2 Methods

### 2.1 Study area

This study focused on the waters of the Banda Sea and Makassar Strait, encompassing approximately 1.68°–8.7° S latitude and 114.88°–134° E longitude (**Fig. 1**). The area is characterized by variable bathymetry, featuring deep ocean basins and narrow continental shelf margins. This region plays a crucial role as a migratory corridor for pelagic fish species, and serves as a significant fishery production zone. Additionally, it constitutes a key segment of the ITF that connects the Pacific and Indian Oceans.

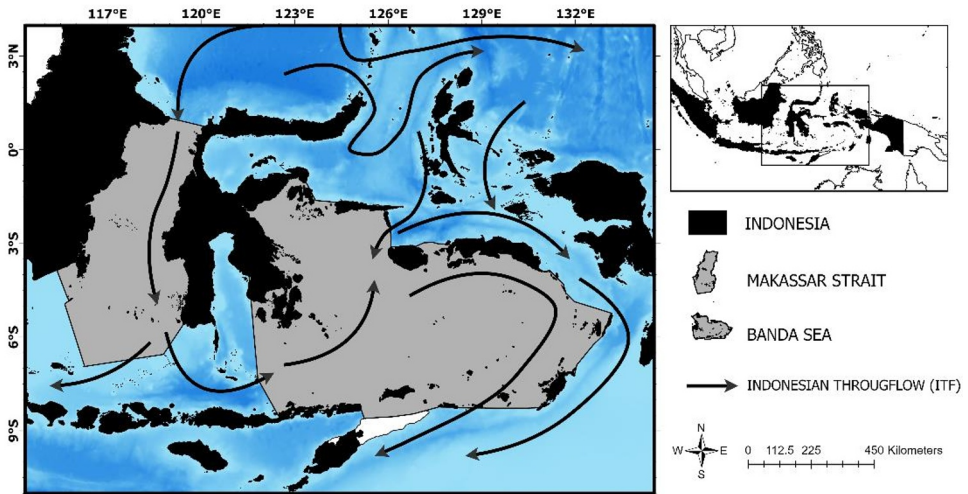


**Fig. 1.** Study area covering the Makassar Strait and the Banda Sea, two key regions in the ITF system. The map displays the geographical boundaries and coordinates used for monitoring the spatial-temporal variability of oceanographic parameters under the influence of ENSO and IOD.

## 2.2 Oceanographic parameters data collection

The oceanographic data used in this study comprised four primary parameters: SST, Chl-a, SSS, CUR. SST and Chl-a data were obtained from the Ocean Color portal (<https://oceancolor.gsfc.nasa.gov/>) as monthly Level-3 composites with a spatial resolution of 4 km, providing consistent temporal coverage for anomaly analysis. SSS and CUR data were sourced from Marine Copernicus (<https://marine.copernicus.eu/>) as monthly averaged products derived from global reanalysis fields with an 8 km spatial resolution. All datasets cover the period 2021–2024, ensuring comparable spatial and temporal resolutions across the parameters.

## 2.3 ENSO and IOD data collection

ENSO and IOD indices were employed to assess the influence of large-scale climate variability on oceanographic conditions in the Banda Sea and the Makassar Strait. The ENSO phase was determined based on monthly Niño 3.4 index values, whereas the IOD was represented by the Dipole Mode Index (DMI). Both datasets were sourced from NOAA Physical Sciences Laboratory (<https://psl.noaa.gov/data/timeseries/month/>).

## 2.4 Anomaly method

The four parameters collected from 2021 to 2024 were used to calculate the anomaly values based on a climatological baseline spanning from 2007 to 2024. The resulting anomalies were then utilized to analyze the relationship between changes in oceanographic conditions and ENSO–IOD variability. The anomaly calculation was defined using the following formula [15]:

$$\delta_{ij} = \bar{T}_{ij} - \bar{T}_i \quad (1)$$

Where  $\delta_{ij}$  represents the oceanographic parameter anomaly (SST, Chl-a, SSS, or CUR) for month  $i$  and year  $j$ ,  $\bar{T}_{ij}$  is the average value of the oceanographic factor for month  $i$  and year  $j$ , and  $\bar{T}_i$  is the climatological average of the factor for month  $i$  over the baseline period.

### 3 Results and discussions

#### 3.1 The characteristics of ENSO and IOD periods (2021-2024)

The analysis of major climate phenomena, namely ENSO and IOD, from 2021 to 2024 identified several dominant phases that serve as the temporal framework for this study (**Table 1**).

**Table 1.** ENSO and IOD periods and phases during the 2021–2024 study period. This table serves as the temporal reference for categorizing oceanographic anomalies analyzed in this study.

| Phenomenon | Phase              | Period                     | Duration (months) | Description                   |
|------------|--------------------|----------------------------|-------------------|-------------------------------|
| ENSO       | La Niña            | August 2021 – January 2023 | 18                | Extreme cooling               |
| ENSO       | Netral             | February 2023 – May 2023   | 4                 | Normal conditions             |
| ENSO       | El Niño            | June 2023 – April 2024     | 11                | Extreme warming               |
| IOD        | Positif (IOD+)     | August 2023 – January 2024 | 6                 | Warming                       |
| IOD        | Negatif dan Netral | -                          | -                 | No cooling, normal conditions |

The extended La Niña period from August 2021 to January 2023 manifested as significant oceanic cooling within the study region, representing a rare multiyear event consistent with the triple-dip La Niña documented during 2020–2023 [16]. Subsequently, a neutral ENSO phase prevailed for approximately four months in early 2023. This event transitioned to a strong El Niño episode from June 2023 to April 2024. Concurrently, a pronounced positive Indian Ocean Dipole (IOD+) occurred between August 2023 and January 2024, coinciding with El Niño and indicating anomalously warm SST in the eastern tropical Indian Ocean. No significant negative IOD (IOD –) events were observed during the study period, suggesting that neutral or warming conditions dominated outside the IOD+ interval.

The determination of ENSO and IOD phase periods is essential as a basis for analyzing the variability of the ITF and oceanographic parameters such as SST, Chl-a, SSS, and CUR in the Makassar Strait and Banda Sea. The warming periods during El Niño and the positive IOD (IOD+) provide a critical context for observing the responses of the oceanographic conditions and ITF dynamics during these intervals.

#### 3.2 Distribution of oceanographic parameter anomalies in the Makassar Strait and Banda Sea during La Niña, El Niño, and IOD periods

##### 3.2.1 Distribution of oceanographic parameters anomalies during the La Niña periods

**Fig. 2** illustrates the spatial distribution of oceanographic parameter anomalies in the Makassar Strait and Banda Sea during the La Niña period. The four primary parameters were SST, Chl-a, SSS, and CUR.

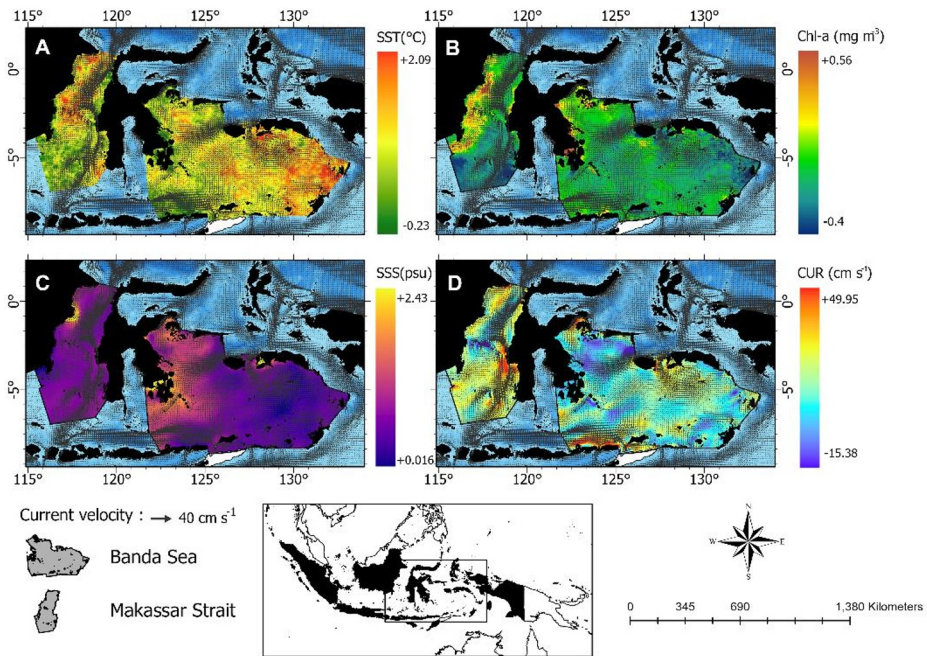


**Fig. 2.** Spatial distribution of oceanographic parameter anomalies in the Makassar Strait and Banda Sea during the La Niña period (August 2021 – January 2023). (A) Spatial distribution of SST anomalies, (B) spatial distribution of Chl-a anomalies, (C) spatial distribution of SSS anomalies, and (D) spatial distribution of CUR anomalies.

The spatial distribution of SST anomalies during the La Niña period (**Fig. 2A**) exhibited widespread red-to-yellow hues throughout nearly the entire study region, indicating notably warmer than normal SST. Dominant warming is particularly evident in the Makassar Strait and the Banda Sea, with peak intensity in the central to southern Banda Sea [6]. Chl-a (**Fig. 2B**) declined across much of the area, as shown by the blue-green shading that marks negative anomalies, with the most pronounced decreases occurring in the eastern and southern Banda Sea, while restricted positive anomalies appeared near the northern Makassar Strait and along the western coast [17]. SSS anomalies (**Fig. 2C**) were predominantly positive, and chemical shifts were the most considerable in the western Banda Sea, with moderate increases in the Makassar Strait. No negative anomalies were detected [18]. The CUR pattern (**Fig. 2D**) revealed relatively strong southward flows in the central to southern Makassar Strait toward the Flores Sea and enhanced CUR in the southern and eastern Banda Sea, forming swirl-like circulations along the basin margins [19].

Overall, these findings show anomalous and extensive warming of regional waters during La Niña. Although La Niña is typically associated with surface cooling in parts of the eastern Indonesian Sea, several local-scale processes may explain the observed warm anomalies. First, La Niña is known to strengthen the ITF, increasing the advection of warm western Pacific waters into both the Makassar Strait and Banda Sea [8]. This enhanced inflow can override the expected surface cooling, particularly in deep-basin regions, where vertical mixing redistributes heat. Second, seasonal dynamics during 2021–2023 multi-year La Niña may have reduced the intensity of wind-driven upwelling in the Banda Sea, limiting the upward supply of cooler subsurface waters [20]. Third, recent studies have documented a long-term increase in ocean heat content across the Maritime Continent [6], which can amplify the background warming during La Niña events. Together, these mechanisms

suggest that the warming observed in this study reflects a combination of strengthened ITF heat transport, altered monsoonal forcing, and broader regional warming trends, offering a plausible explanation for the deviation from canonical ENSO expectations.

### 3.2.2 Distribution of oceanographic parameters anomalies during the El Niño periods

During the El Niño period (**Fig. 3A**), the spatial distribution of SST anomalies deviated from the canonical pattern typically observed in eastern Indonesia. Warm anomalies, depicted by red–yellow shading, were concentrated in the southern Makassar Strait and the western sector of the study area, whereas much of the Banda Sea exhibited muted green tones, indicative of weakly positive or near-neutral SST anomalies. Localized warming was confined to the southeastern Banda Sea, whereas the central and northern sectors largely maintained neutral conditions [12]. Chl-a concentrations (**Fig. 3B**) generally declined across most of the region, as indicated by blue–green shading, which represents negative anomalies. The strongest decreases occurred in the eastern and central Banda Sea, whereas slight increases in the northern Makassar Strait were likely linked to nutrient inputs from the Sulawesi Sea [16, 17]. SSS anomalies (**Fig. 3C**) were predominantly positive, marked by purple–pink tones, with peak values in the eastern Banda Sea and moderate anomalies in the western Makassar Strait. Negative anomalies are absent during this phase [5]. The CUR (**Fig. 3D**) intensified noticeably in the central to northern Makassar Strait. In the Banda Sea, elevated CUR trace the southern and eastern margins, forming circular circulation features, a pattern consistent with satellite-observed Chl-a dynamics influenced by the ENSO in the broader Indonesian seas [14]. Overall, El Niño observed during the study period generated localized rather than widespread warming, with much of the Banda Sea remaining thermally neutral. This suggests that the impact of El Niño on SST in the region may have been attenuated by local oceanographic and atmospheric factors, including variations in CUR dynamics and inter-basin water mass exchanges [5].

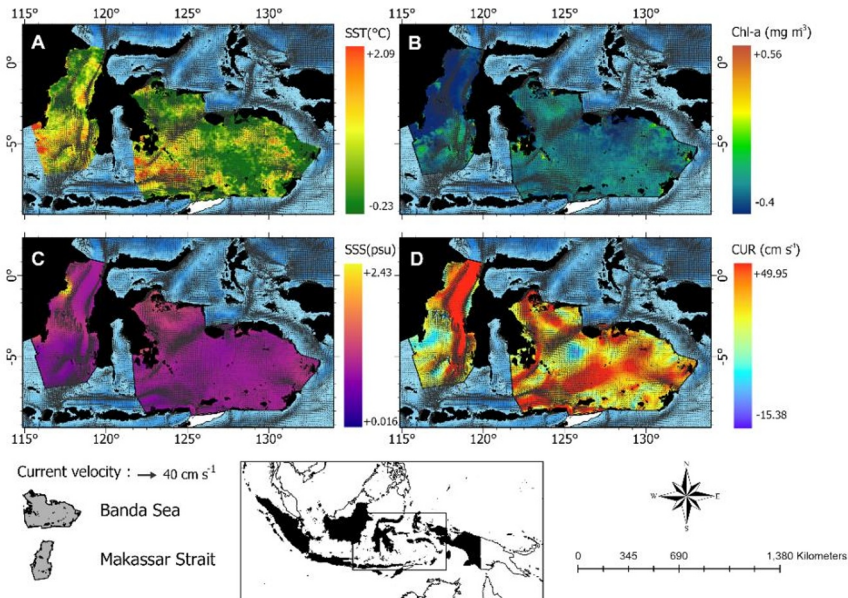


**Fig. 3.** Spatial distribution of oceanographic parameter anomalies in the Makassar Strait and Banda Sea during the El Niño period (June 2023 – April 2024). (A) Spatial distribution of SST anomalies, (B) spatial distribution of Chl-a anomalies, (C) spatial distribution of SSS anomalies, and (D) spatial distribution of CUR anomalies.

### 3.2.3 Distribution of oceanographic parameters anomalies during the IOD+

During the positive Indian Ocean Dipole (IOD+) period (**Fig. 4A**), the spatial distribution of SST anomalies exhibited pronounced east–west contrasts. Positive anomalies (red–yellow shading) were concentrated in the western Makassar Strait and off eastern Borneo, whereas the Banda Sea and adjacent eastern areas predominantly showed green coloration, indicating neutral to slightly negative anomalies. The most intense warming occurred in the western Makassar Strait and offshore eastern Kalimantan [4]. Chl-a (**Fig. 4B**) mostly declined across the Banda Sea, as evidenced by blue–green hues denoting negative anomalies, whereas positive anomalies appeared near the south-eastern coast of Sulawesi. SST-driven biological perturbations, including suppressed Chl-a levels during IOD+ in eastern maritime regions, have been well documented [4]. During the positive Indian Ocean Dipole (IOD+) period (**Fig. 4C**), SSS anomalies were predominantly positive across nearly the entire study area, marked by purple–pink shading. The highest SSS anomalies were uniformly observed in the Banda Sea, whereas the Makassar Strait exhibited moderately elevated SSS values. These observations align with the regional SSS structures during IOD+ events, where advective processes contribute to basin-wide SSS increases [21]. Moreover, SSS anomalies have been shown to persist into the decay phase of IOD+, even after the SST anomalies subsided [22]. CUR patterns (**Fig. 4D**) revealed intensified flow along the Makassar Strait toward the Flores Sea and strong CUR with contour-following circulation in the central and western Banda Sea, which are consistent with IOD-modulated dynamics, such as altered upwelling and ITF transport [11]. In summary, the IOD+ period featured marked warming in western marine zones (notably the Makassar Strait), along with neutral to slightly cooler waters in the eastern Banda Sea. These conditions coincided with uniformly elevated SSS and largely suppressed the Chl-a concentrations in the eastern region. This spatial pattern suggests a strong local response modulated by oceanographic drivers such as upwelling suppression and ITF adjustments during IOD+ events.

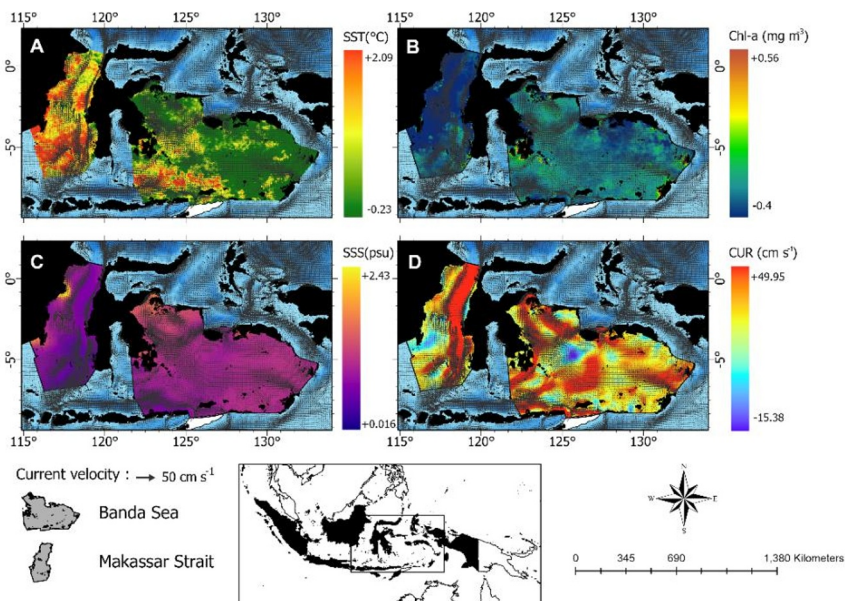


**Fig. 4.** Spatial distribution of oceanographic parameter anomalies in the Makassar Strait and Banda Sea during the IOD+ period (August 2023 – January 2024). (A) Spatial distribution of SST anomalies, (B) spatial distribution of Chl-a anomalies, (C) spatial distribution of SSS anomalies, and (D) spatial distribution of CUR anomalies.

### 3.3 Relationship between ENSO-IOD and oceanographic parameter anomalies

#### 3.3.1 Relationship between ENSO-IOD and SST anomalies

During the La Niña period, SST anomalies in the Banda Sea and Makassar Strait were generally positive, with mean values of  $+0.48^{\circ}\text{C}$  and  $+0.266^{\circ}\text{C}$ , respectively (**Fig. 5**). This warming can be explained by regional oceanographic processes that are unique to eastern Indonesia. La Niña typically strengthens the ITF, increasing the transport of warm western Pacific waters into the Makassar Strait and, subsequently, into the Banda Sea. This enhanced warm-water advection can dominate localized cooling processes and lead to positive SST anomalies, particularly in deep-basin environments where vertical mixing redistributes heat more efficiently [23]. In addition, the multi-year 2021-2023 La Niña event may have contributed to the sustained accumulation of ocean heat content across the maritime continent, reinforcing surface warming in both regions.

During the El Niño period, concurrent with a positive Indian Ocean Dipole (IOD+), the SSTs in both the Banda Sea and Makassar Strait also increased, with mean anomalies of  $+0.099^{\circ}\text{C}$  and  $+0.176^{\circ}\text{C}$ , respectively. This pattern is consistent with a reduction in the warm water supply from the Pacific due to ITF weakening combined with enhanced thermal stratification that inhibits vertical mixing and allows surface layers to warm more rapidly [24]. Although El Niño is typically associated with drier conditions and reduced cloud cover, the resulting increase in incoming solar radiation can further amplify surface warming [25], particularly in the Banda Sea, which is highly sensitive to variations in regional circulation and surface heat fluxes.

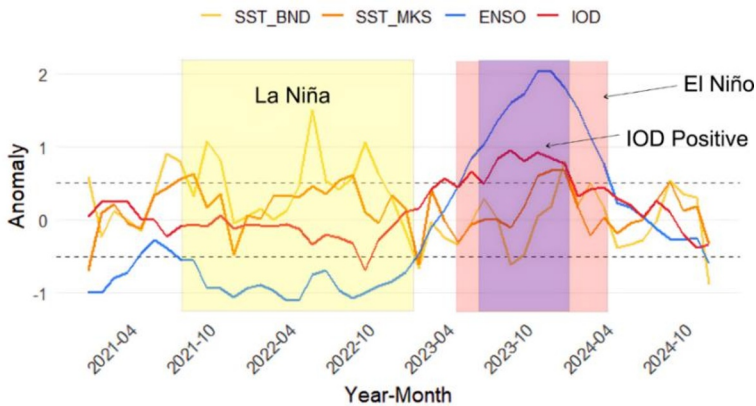


**Fig. 5.** Graph illustrating the relationship between ENSO-IOD indices and SST anomalies in the Makassar Strait and Banda Sea. This visualization shows the temporal thermal response of the study areas to global climate forcing.

#### 3.3.2 Relationship between ENSO-IOD and Chl-a anomalies

Based on **Fig. 6**, the pattern of the relationship between ENSO and IOD and Chl-a concentration anomalies in the Banda Sea and Makassar Strait exhibit variations that correspond closely with changes in global climate phases.

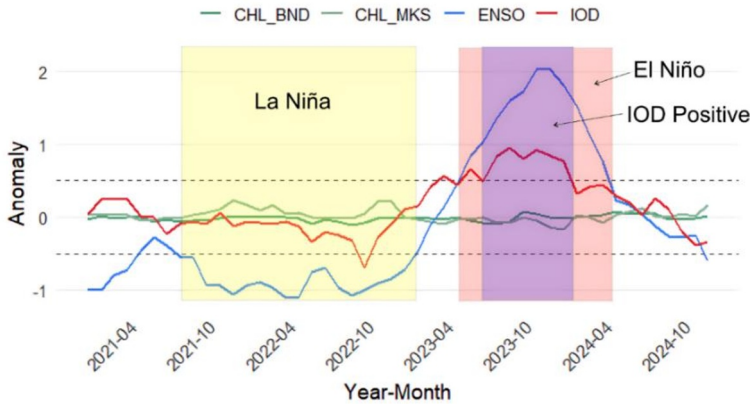


**Fig. 6.** Graph illustrating the relationship between ENSO-IOD indices and Chl-a anomalies in the Makassar Strait and Banda Sea. The data highlights how climate-driven changes affect phytoplankton biomass and primary productivity in these regions.

During the La Niña period, the ENSO index exhibited predominantly negative anomalies with an average anomaly of  $-0.887^{\circ}\text{C}$ , whereas the Indian Ocean Dipole (IOD) remained largely neutral. In the Banda Sea, Chl-a anomalies tended to be negative, averaging  $-0.032\text{ mg m}^{-3}$ , except between December 2021 and February 2022, when a slight increase of  $+0.0026$  to  $+0.0102\text{ mg m}^{-3}$  was observed. Conversely, in the Makassar Strait, Chl-a anomalies during La Niña were predominantly positive, with a mean value of  $+0.077\text{ mg m}^{-3}$ . This suggests that La Niña exerts a stronger influence on Chl-a concentrations in the Makassar Strait than in the Banda Sea, likely because of the role of the ITF, whose main inflow pathway is through the Makassar Strait [26]. During the El Niño and positive IOD (IOD+) phases, ENSO exhibited strong positive anomalies, peaking in November–December 2023 at  $+2^{\circ}\text{C}$ , while the IOD index also increased, averaging  $+0.85^{\circ}\text{C}$ . In the Banda Sea, Chl-a anomalies were predominantly negative, with an average of  $-0.0172\text{ mg m}^{-3}$ , indicating reduced primary productivity, likely driven by elevated SST and weakened vertical mixing, which diminished the nutrient supply to surface waters [27]. A similar pattern occurred in the Makassar Strait, where negative Chl-a anomalies were observed during the peak of the El Niño–IOD+ event, suggesting that the combined influence of these climate modes significantly reduced the phytoplankton biomass, although the magnitude of the decline was smaller than that in the Banda Sea. During transitional periods, either between La Niña and El Niño or following the decay of El Niño, Chl-a anomalies in both regions were generally negative. This pattern is likely influenced by local factors, such as the onset of the northwest monsoon, which brings low-nutrient waters, and the advection of oligotrophic Pacific waters via the ITF, both of which naturally suppress phytoplankton productivity [11].

### 3.3.3 Relationship between ENSO-IOD and SSS anomalies

During the La Niña period, SSS anomalies in the Makassar Strait were generally positive, with a mean value of  $+0.07\text{ psu}$  (Fig. 7). The Banda Sea also exhibited predominantly positive anomalies, although with greater fluctuations averaging  $+0.131\text{ psu}$ . This increase in SSS is likely influenced by the intensified inflow of high SSS water masses from the western Pacific through the ITF. This condition is consistent with enhanced ITF transport during La Niña, which strengthens the supply of saline water to the eastern Indonesian seas [11]. During El Niño coinciding with a positive Indian Ocean Dipole (IOD+), the SSS anomalies in the two regions exhibited contrasting patterns. In the Banda Sea, SSS anomalies were predominantly positive, with a mean increase of  $+0.377\text{ psu}$ . In contrast, the Makassar Strait exhibited more

variable conditions, including a temporary negative anomaly during the mid-phase of El Niño events. However, the overall mean value remains positive at +0.344 psu. This pattern suggests a reduction in saline water supply from the Pacific due to weakened ITF transport, combined with possible influences from rainfall variability and increased local freshwater input [28]. The differences in SSS responses between the Banda Sea and Makassar Strait indicate that ENSO–IOD impacts are not solely governed by large-scale ocean circulation, but are also modulated by local processes, such as precipitation–evaporation balance, riverine discharge, and inter-basin water exchange within eastern Indonesia [29].

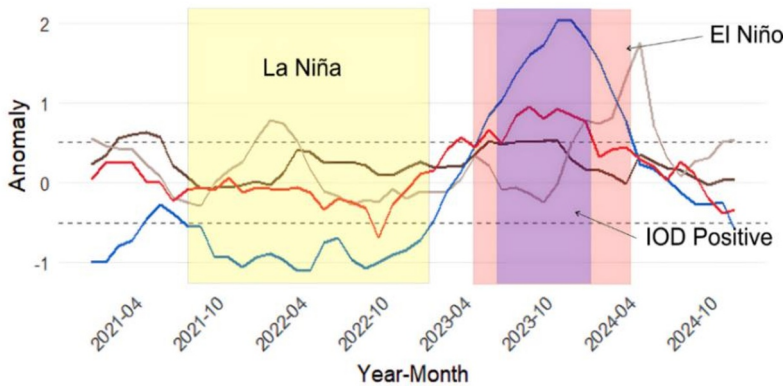


**Fig. 7.** Graph illustrating the relationship between ENSO-IOD indices and SSS anomalies in the Makassar Strait and Banda Sea. The plot shows the temporal variations in surface salinity and its response to freshwater flux changes driven by climate events during the study period.

### 3.3.4 Relationship between ENSO-IOD and CUR anomalies

During the La Niña period, the CUR anomalies in the Makassar Strait were predominantly negative with a mean value of  $-1.334 \text{ cm s}^{-1}$  (**Fig. 8**). In contrast, the Banda Sea displayed more variable anomalies, although most were positive, averaging  $+0.568 \text{ cm s}^{-1}$ . This pattern suggests the influence of local CUR intensification in the Banda Sea, likely driven by regional circulation patterns and monsoonal wind forcing in eastern Indonesia [23]. During the 2023 El Niño event, coinciding with a positive Indian Ocean Dipole (IOD+), both locations exhibited positive CUR anomalies, with mean values of  $+4.947 \text{ cm s}^{-1}$  in the Banda Sea and  $+6.516 \text{ cm s}^{-1}$  in the Makassar Strait. This indicates a significant strengthening of CUR, likely caused by an increased sea level gradient between the western Pacific and eastern Indian Ocean, thereby enhancing the ITF through these passages [8]. Overall, the ENSO–IOD relationship with CUR in this study revealed that La Niña was associated with weakened surface flow in the Makassar Strait and enhanced CUR in the Banda Sea, whereas El Niño–IOD+ conditions tended to strengthen CUR in both regions. This finding highlights the complex interplay between large-scale climate modes and local oceanographic processes in modulating CUR variability in the Indonesian seas.

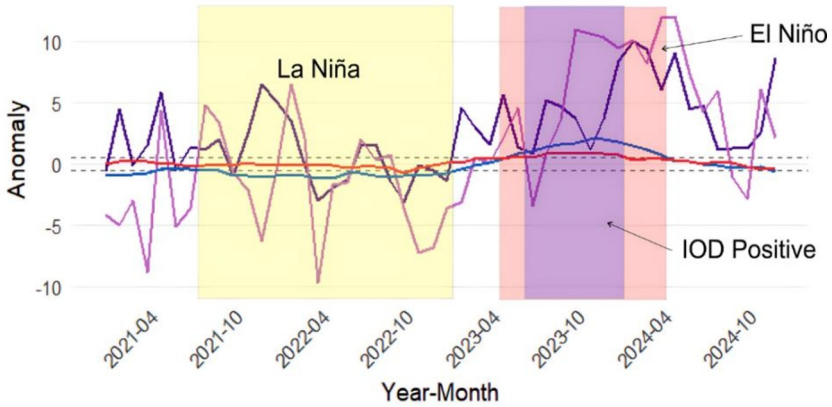


**Fig. 8.** Graph illustrating the relationship between ENSO-IOD indices and CUR anomalies in the Makassar Strait and Banda Sea. The comparison highlights the intensification or weakening of the Indonesian Throughflow (ITF) speed in response to global climate forcing.

### 3.4 Correlation analysis between ENSO-IOD and oceanographic parameter anomalies

Based on the results of the correlation analysis (**Fig. 9**), most of the oceanographic parameter anomalies exhibited strong interrelationships. Additionally, correlations between ENSO and IOD indices and oceanographic anomalies also demonstrated significant associations.

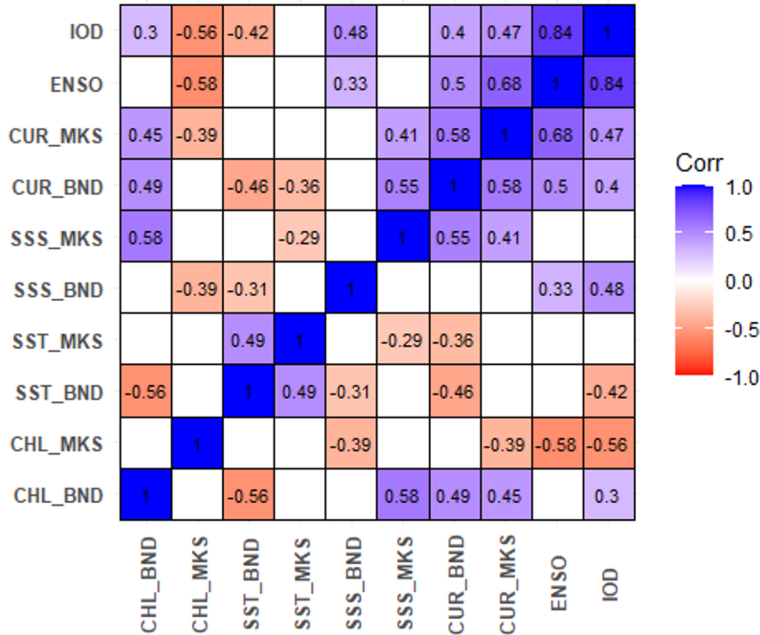


**Fig. 9.** Correlation matrix between ENSO-IOD indices and oceanographic parameter anomalies in the Makassar Strait and Banda Sea. This visualization highlights the significance of regional responses to climate forcing, showing how ENSO and IOD specifically influence the variability of the ITF corridors.

**Fig. 9** presents the results of Pearson's correlation coefficient ( $r$ ) analysis to assess the strength and direction of the linear relationship between the two quantitative variables. The  $r$  values range from  $-1$  to  $+1$ , where values approaching  $+1$  indicate a strong positive correlation (an increase in one variable is accompanied by an increase in the other), whereas values approaching  $-1$  indicate a strong negative correlation (an increase in one variable is accompanied by a decrease in the other). Values of  $r$  near zero suggest the absence of a significant linear relationship between variables.

In statistical analysis, the  $p$ -value represents the probability of obtaining results at least as extreme as those observed, assuming that the null hypothesis is true. A  $p$ -value below the conventional threshold of  $0.05$  indicates a statistically significant relationship, implying that the likelihood of the observed association occurring by chance is low. Conversely, a  $p$ -value equal to or greater than  $0.05$  suggests insufficient evidence to reject the null hypothesis [30]. This interpretation is essential to ensure that the relationships identified between the variables in the present study are meaningful and are not the result of random variability in the dataset. Pearson's correlation analysis revealed moderate-to-strong associations between several variable pairs. The Chl-a concentrations in the Banda Sea (CHL\_BND) exhibited a moderate positive correlation with SSS in the Makassar Strait ( $r = 0.58$ ,  $p = 0.0000163$ ), as well as with CUR in both the Banda Sea ( $r = 0.49$ ,  $p = 0.000351$ , approaching the moderate threshold) and the Makassar Strait (CUR\_MKS;  $r = 0.45$ ,  $p = 0.00147$ ). In contrast, Chl-a in the Makassar Strait showed a strong negative correlation with the El Niño–Southern Oscillation (ENSO) index ( $r = -0.58$ ,  $p = 0.0000157$ ) and a moderate negative correlation with the Indian Ocean Dipole (IOD) index ( $r = -0.56$ ,  $p = 0.0000407$ ), indicating a significant influence of large-scale climate variability on primary productivity in this region [31]. SST in the Banda Sea was moderately and negatively correlated with Chl-a ( $r = -0.56$ ,  $p = 0.0000326$ ), suggesting that warmer surface waters are generally associated with lower phytoplankton biomass, possibly because of stratification effects that reduce nutrient availability. SSS in the Makassar Strait displayed moderate positive correlations with CUR in both the Banda Sea ( $r = 0.55$ ,  $p = 0.0000567$ ) and the Makassar Strait ( $r = 0.41$ ,  $p = 0.00336$ , approaching moderate strength). The CUR in these two regions were moderately to strongly correlated ( $r = 0.58$ ,  $p = 0.0000163$ ), reflecting the interconnected nature of the Banda–Makassar circulation patterns. ENSO and IOD indices exhibited a very strong positive correlation ( $r = 0.84$ ,  $p = 5.17 \times 10^{-14}$ ), consistent with the known coupling of these two major climate modes [32]. The analysis further indicated that ENSO was moderately and negatively correlated with Chl-a in the Makassar Strait ( $r = -0.58$ ,  $p = 0.00000157$ ), implying that strong El Niño events tend to suppress phytoplankton productivity, likely because of the reduced nutrient supply from upwelling. Moreover, ENSO showed a strong positive correlation with CUR in the Makassar Strait ( $r = 0.68$ ,  $p = 1.15 \times 10^{-7}$ ) (**Fig. 9; Table 2**), indicating that higher ENSO indices are associated with stronger CUR. This pattern may be linked to shifts in the pressure gradients and large-scale circulation during ENSO events [10].

**Table 2.** P-values from statistical tests between selected oceanographic parameter anomalies and ENSO–IOD indices. Values below  $0.05$  indicate a statistically significant correlation between climate drivers and regional oceanographic changes.

|         | CHL_BND  | CHL_MKS  | SST_BND  | SST_MKS  | SSS_BND  | SSS_MKS  | CUR_BND  | CUR_MKS  | ENSO     | IOD      |
|---------|----------|----------|----------|----------|----------|----------|----------|----------|----------|----------|
| CHL_BND | NA       | 1.84E-01 | 3.26E-05 | 0.090989 | 0.892497 | 1.63E-05 | 3.51E-04 | 1.47E-03 | 9.25E-02 | 3.54E-02 |
| CHL_MKS | 1.84E-01 | NA       | 8.32E-01 | 0.052759 | 0.00626  | 6.19E-01 | 4.87E-01 | 5.46E-03 | 1.57E-05 | 4.07E-05 |
| SST_BND | 3.26E-05 | 8.32E-01 | NA       | 0.000457 | 0.030782 | 9.86E-02 | 8.79E-04 | 1.56E-01 | 8.22E-02 | 2.94E-03 |
| SST_MKS | 9.10E-02 | 5.28E-02 | 4.57E-04 | NA       | 0.779805 | 4.44E-02 | 1.32E-02 | 3.55E-01 | 6.24E-01 | 8.40E-01 |
| SSS_BND | 8.92E-01 | 6.26E-03 | 3.08E-02 | 0.779805 | NA       | 4.44E-01 | 5.13E-01 | 8.01E-01 | 2.19E-02 | 5.74E-04 |

|         | CHL_BND  | CHL_MKS  | SST_BND  | SST_MKS  | SSS_BND  | SSS_MKS  | CUR_BND  | CUR_MKS  | ENSO     | IOD      |
|---------|----------|----------|----------|----------|----------|----------|----------|----------|----------|----------|
| SSS_MKS | 1.63E-05 | 6.19E-01 | 9.86E-02 | 0.044444 | 0.444449 | NA       | 5.67E-05 | 3.36E-03 | 2.91E-01 | 2.98E-01 |
| CUR_BND | 3.51E-04 | 4.87E-01 | 8.79E-04 | 0.013204 | 0.512599 | 5.67E-05 | NA       | 1.63E-05 | 3.11E-04 | 5.26E-03 |
| CUR_MKS | 1.47E-03 | 5.46E-03 | 1.56E-01 | 0.354947 | 0.800885 | 3.36E-03 | 1.63E-05 | NA       | 1.15E-07 | 7.39E-04 |
| ENSO    | 9.25E-02 | 1.57E-05 | 8.22E-02 | 0.624171 | 0.021931 | 2.91E-01 | 3.11E-04 | 1.15E-07 | NA       | 5.17E-14 |
| IOD     | 3.54E-02 | 4.07E-05 | 2.94E-03 | 0.839734 | 0.000574 | 2.98E-01 | 5.26E-03 | 7.39E-04 | 5.17E-14 | NA       |

## 4 Conclusion

This study investigates the influence of the El Niño-Southern Oscillation (ENSO) and Indian Ocean Dipole (IOD) on oceanographic anomalies in the Makassar Strait and Banda Sea, two critical corridors of the ITF, from 2021 to 2024. This analysis examines the spatial distribution of SST, Chl-a, SSS, and CUR anomalies during distinct ENSO and IOD phases. During La Niña, the Banda Sea exhibited negative Chl-a anomalies, whereas the Makassar Strait showed positive anomalies. During El Niño and a positive IOD (IOD+), both regions experienced negative Chl-a anomalies, with a more pronounced decline in the Banda Sea. SST anomalies were generally positive during La Niña and localized during El Niño and IOD+. The SSS anomalies were predominantly positive during La Niña and El Niño–IOD+, with higher anomalies in the Banda Sea. CUR exhibited weakened flow in the Makassar Strait and intensified CUR in the Banda Sea during La Niña, whereas El Niño–IOD+ conditions strengthened the CUR in both regions. Correlation analysis revealed significant relationships between the ENSO and IOD indices and oceanographic anomalies, highlighting the complex interplay between large-scale climate modes and local processes in modulating the variability of the ITF and associated oceanographic parameters.

We acknowledge the PMDSU Scholarship Program of the Ministry of Higher Education, Research, and Technology of the Republic of Indonesia for funding this study.

## References

- 1 A. Santoso, M.H. England, J.B. Kajtar, W. Cai, Indonesian throughflow variability and linkage to ENSO and IOD in an ensemble of CMIP5 models. *J. Clim.* **35**, 3161–3178 (2022). <https://doi.org/10.1175/JCLI-D-21-0485.1>
- 2 N.A. Azuga, A.D. Habibullah, Interannual variability of sea level anomaly (sla) in the Western Sumatra coastal waters driven by ENSO and IOD modulations. *Asian J. Aquat. Sci.* **7**, 422–431 (2024). <https://doi.org/10.31258/ajoa.7.3.422-431>
- 3 R. Furue, M. Nonaka, H. Sasaki, The intrinsic variability of the Indonesian Throughflow. *Front. Mar. Sci.* **10**, 1–17 (2023). <https://doi.org/10.3389/fmars.2023.1117304>
- 4 A. Li, Y. Zhang, M. Hong, J. Shi, J. Wang, Relative importance of ENSO and IOD on interannual variability of Indonesian Throughflow transport. *Front. Mar. Sci.* **10**, 1–16, (2023). <https://doi.org/10.3389/fmars.2023.1182255>
- 5 K.R. Pratama, I.M. Radjawane, B.E. Pratama, Effect of El-Niño Southern Oscillation (ENSO) on heat transport in the Indonesia Throughflow passages and ocean heat content in the Banda Sea. *J. Indones. Trop. Anim. Agric.* **30**, 92–102 (2025). <https://doi.org/10.14710/ik.ijms.30.1.92-102>
- 6 Y. Jin, Y. Li, L. Cheng, J. Duan, R. Li, F. Wang, Ocean heat content increase of the

- maritime continent since the 1990s. *Geophys. Res. Lett.* **51**, 1–10, (2024).  
<https://doi.org/10.1029/2023GL107526>
- 7 M. Fritz, M. Mayer, L. Haimberger, S. Winkelbauer, Assessment of Indonesian Throughflow transports from ocean reanalyses with mooring-based observations. *Ocean Sci.* **19**, 1203–1223 (2023). <https://doi.org/10.5194/os-19-1203-2023>
  - 8 S. Hu, J. Sprintall, Interannual variability of the Indonesian Throughflow: The salinity effect. *J. Geophys. Res. Ocean.* **121**, 2596–2615 (2016).  
<https://doi.org/10.1002/2015JC011495>
  - 9 M.Z. Lubis, E. Situmorang, A.V.H. Simanjuntak, N.F. Riama, G.R. Pasma, A. Dwinovantyo, H. Kausarian, N.M.N. Natih, Batara, K. Ansari, P. Jamjareegulgarn, Indonesian Throughflow, spatial–temporal variability, and its relationship to ENSO events in the Lombok Strait. *Egypt. J. Aquat. Res.* **51**, 7–18 (2025).  
<https://doi.org/10.1016/j.ejar.2025.01.004>
  - 10 J. Sprintall, A.L. Gordon, A. Koch-Larrocy, T. Lee, J.T. Potemra, K. Pujiana, S.E. Wijffels, The Indonesian seas and their role in the coupled ocean–climate system. *Nat. Geosci.* **7**, 487–492 (2014). <https://doi.org/10.1038/ngeo2188>
  - 11 J. Sprintall, A.L. Gordon, S.E. Wijffels, M. Feng, S. Hu, A. Koch-Larrocy, H. Phillips, D. Nugroho, A. Napitu, K. Pujiana, R.D. Susanto, B. Sloyan, B. Peña-Molino, D. Yuan, N.F. Riama, S. Siswanto, A. Kuswardani, Z. Arifin, A.J. Wahyudi, H. Zhou, T. Nagai, J.K. Ansong, R. Bourdalle-Badié, J. Chanut, F. Lyard, B.K. Arbic, A. Rahmdhani, A. Setiawan, Detecting change in the Indonesian seas. *Front. Mar. Sci.* **6**, 1–24 (2019). <https://doi.org/10.3389/fmars.2019.00257>
  - 12 U.O. Nurafifah, M. Zainuri, A. Wirasatriya, Pengaruh ENSO dan IOD terhadap distribusi suhu permukaan laut dan klorofil-a pada periode upwelling di laut Banda. *Indones. J. Oceanogr.* **4**, 74–85 (2022). <https://doi.org/10.14710/ijoce.v4i3.14971>
  - 13 Y.D. Haryanto, H. Hadiman, R. Agdialta, N.F. Riama, Pengaruh El Niño terhadap pola distribusi klorofil-a dan pola arus di wilayah perairan Selatan Maluku. *J. Kelaut. Trop.* **24**, 364–374 (2021). <https://doi.org/10.14710/jkt.v24i3.10456>
  - 14 F. Simanjuntak, T.H. Lin, Monsoon effects on chlorophyll-a, sea surface temperature, and ekman dynamics variability along the Southern Coast of Lesser Sunda Islands and its Relation to ENSO and IOD based on satellite observations. *Remote Sens.* **14**, 1–28 (2022). <https://doi.org/10.3390/rs14071682>
  - 15 H.A. Andrade, C.A.E. Garcia, Skipjack tuna fishery in relation to sea surface temperature off the southern Brazilian coast. *Fish. Oceanogr.* **8**, 245–254 (1999).  
<https://doi.org/10.1046/j.1365-2419.1999.00107.x>
  - 16 X. Li, Z.Z. Hu, M.J. McPhaden, C. Zhu, Y. Liu, Triple-dip La Niñas in 1998–2001 and 2020–2023: impact of mean state changes. *J. Geophys. Res. Atmos.* **128**, 1–16 (2023).  
<https://doi.org/10.1029/2023JD038843>
  - 17 A. Bahtiar, Yulfiah, Impacts of La Niña on sea surface temperature, chlorophyll-a, and fishery productivity in Northern East Java Ocean. *J. Earth Mar. Technol.* **5**, 171–183 (2025). <https://doi.org/10.31284/j.jemt.2025.v5i2.7905>
  - 18 A. Bahiyah, A. Wirasatriya, W. Mardiansyah, I. Iskandar, An updated water masses stratification of Indonesian maritime continent (IMC) attributed to normal and ENSO conditions by argo float. *Sci. Technol. Indones.* **9**, 299–313 (2024).  
<https://doi.org/10.26554/sti.2024.9.2.299-313>
  - 19 A.L. Gordon, A. Napitu, B.A. Huber, L.K. Gruenburg, K. Pujiana, T. Agustiadi, A. Kuswardani, N. Mbay, A. Setiawan, Makassar strait throughflow seasonal and interannual variability: an overview. *J. Geophys. Res. Ocean.* **124**, 3724–3736 (2019).

- <https://doi.org/10.1029/2018JC014502>
- 20 J. Sprintall, J.T. Potemra, S.L. Hautala, N.A. Bray, W.W. Pandoe, Temperature and salinity variability in the exit passages of the Indonesian Throughflow. *Deep. Res. Part II Top. Stud. Oceanogr.* **50**, 12–13, 2183–2204 (2003). [https://doi.org/10.1016/S0967-0645\(03\)00052-3](https://doi.org/10.1016/S0967-0645(03)00052-3)
  - 21 S. Kido, T. Tozuka, W. Han, Anatomy of salinity anomalies associated with the positive Indian Ocean Dipole. *J. Geophys. Res. Ocean.* **124**, 8116–8139 (2019). <https://doi.org/10.1029/2019JC015163>
  - 22 Q. Sun, Y. Zhang, Y. Du, X. Jiang, Asymmetric response of sea surface salinity to extreme positive and negative Indian Ocean Dipole in the southern tropical Indian Ocean. *J. Geophys. Res. Ocean.* **127**, 1–15 (2022). <https://doi.org/10.1029/2022JC018986>
  - 23 A.L. Gordon, A. Napitu, B.A. Huber, L.K. Gruenburg, K. Pujiana, The Indonesian Throughflow during 2004–2006 as observed by the INSTANT program. *Dyn. Atmos. Ocean.* **50**, 115–128 (2010). <https://doi.org/10.1016/j.dynatmoce.2009.12.002>
  - 24 Q.Y. Liu, M. Feng, D. Wang, S. Wijffels, Interannual variability of the Indonesian Throughflow transport: A revisit based on 30-year expendable bathythermograph data. *J. Geophys. Res. Ocean.* **120**, 8270–8282 (2015). <https://doi.org/10.1002/2015JC011351>
  - 25 E. Siswanto, T. Horii, I. Iskandar, J.L. Gaol, R.Y. Setiawan, R.D. Susanto, Impacts of climate changes on the phytoplankton biomass of the Indonesian Maritime Continent. *J. Mar. Syst.* **212**, 1–15 (2020). <https://doi.org/10.1016/j.jmarsys.2020.103451>
  - 26 R.D. Susanto, A.L. Gordon, Q. Zheng, Upwelling along the coast of Java and Sumatra and its relation to ENSO. *Geophys. Res. Lett.* **28**, 1599–1602 (2001). <https://doi.org/10.1029/2000GL011844>
  - 27 X. Ding, J. Liu, H. Zhang, Z. Ke, J. Li, W. Liu, K. Li, C. Zhao, Y. Tan, Phytoplankton community patterns in the northeastern South China Sea: implications of intensified Kuroshio intrusion during the 2015/16 El Niño. *J. Geophys. Res. Ocean.* **127**, 1–17 (2022). <https://doi.org/10.1029/2021JC017998>
  - 28 J. Li, Y. Li, Y. Guo, G. Li, F. Wang, Decadal variability of sea surface salinity in the southeastern Indian Ocean: roles of local rainfall and the Indonesian Throughflow. *Front. Mar. Sci.* **9**, 1–18 (2023). <https://doi.org/10.3389/fmars.2022.1097634>
  - 29 E.A. Kisnarti, N.S. Ningsih, M.R. Putri, N. Hendiarti, Current dynamics and water column stability in Indonesian waters based on hydrodynamics model. *Indones. J. Oceanogr.* **52**, 2, 206–215 (2021). <https://doi.org/10.23959/sfdorj-1000010>
  - 30 J.H. Zar, *Biostatistical Analysis* Fifth Edition (Pearson, New Jersey, 2014)
  - 31 E.Y. Handoko, M.A. Syariz, N. Hayati, M. Putri, M. Muryono, C.Y. Kuo, The spatial–temporal variability of chlorophyll-a across the eastern Indonesian seas region using Sentinel-3 OLCI. *Appl. Geomatics.* **16**, 4, 897–904 (2024). <https://doi.org/10.1007/s12518-024-00590-7>
  - 32 G. Meyers, P. McIntosh, L. Pigot, M. Pook, The years of El Niño, La Niña and interactions with the tropical Indian Ocean. *J. Clim.* **20**, 2872–2880 (2007). <https://doi.org/10.1175/JCLI4152.1>